Oil & Gas Science and Technology – Rev. IFP Energies nouvelles, Vol. 66 (2011), No. 4, pp. 667-679

DOI: 10.2516/ogst/2011106

IFP Energies nouvelles International Conference
Rencontres Scientifiques d'IFP Energies nouvelles

E-COSM'09 - IFAC Workshop on Engine and Powertrain Control, Simulation and Modeling
E-COSM'09 - Colloque IFAC sur le contrôle, la simulation et la modélisation des moteurs et groupes motopropulseurs

Persistent Memory Effects and the Mid- and Post-Brick Dynamic Behaviour of Three-Way Automotive Catalysts

J.C. Peyton Jones* and R. Schallock

Center for Nonlinear Dynamics & Control, Villanova University, Villanova PA 19085 - USA
e-mail: james.peyton-jones@villanova.edu - robert.schallock@gmail.com

* Corresponding author

Résumé — Effets mémoires persistants et comportement dynamique des briques médiane et postérieure de catalyseurs automobiles à trois voies — Cet article présente les résultats d'une étude expérimentale en matière de comportement dynamique d'un catalyseur automobile à trois voies et de ses capteurs d'oxygène de gaz d'échappement associés. Motivée par les problèmes de localisation des capteurs de retour d'information, l'étude cherche à corréler les résultats d'expériences répétées, capteurs et analyseurs de gaz à réponse rapide étant disposés en des emplacements différents afin d'obtenir une image détaillée des dynamiques de système en différents points à l'intérieur du catalyseur. Les résultats initiaux ont démontré que la réponse dynamique du catalyseur peut être significativement affectée par un effet mémoire persistant en plus des dynamiques de désactivation réversibles et des dynamiques de stockage/libération d'oxygène familières du système. En particulier, les effets d'un fonctionnement préalable riche ou stœchiométrique s'avèrent persister y compris après des périodes prolongées de fonctionnement pauvre. Cet effet mémoire est important, non seulement du fait de son influence potentielle sur l'efficacité de conversion, mais aussi du fait de son influence sur la répétabilité d'expériences exécutées dans des conditions de fonctionnement qui apparaîtraient comme étant proches de l'identique. Par un pré-conditionnement dans des conditions riches, des expériences hautement répétables ont été obtenues. Les résultats ont été combinés pour offrir une image détaillée des dynamiques de catalyseurs à des emplacements amont, médian et aval par rapport aux catalyseurs, et fournir un aperçu en matière de comportement de catalyseurs et de capteurs d'oxygène de gaz d'échappement (non idéal).

Abstract — Persistent Memory Effects and the Mid- and Post-Brick Dynamic Behaviour of Three-Way Automotive Catalysts — *This paper presents the results of an experimental study into the dynamic behaviour of a three-way automotive catalyst and its associated exhaust gas oxygen sensors. Motivated by issues of feedback sensor location, the study seeks to overlay the results of repeat experiments, with sensors and fast-response gas analyzers positioned at different locations, in order to obtain a detailed picture of system dynamics at different points within the catalyst. Initial results demonstrated that the dynamic response of the catalyst can be significantly affected by a persistent memory effect in addition to reversible deactivation dynamics and the familiar oxygen storage/release dynamics of the system. In particular, the effects of prior rich or stoichiometric operation are shown to persist even after extended periods of lean operation. This memory effect is important, not only because of its potential impact on conversion efficiency, but also because of its impact on the repeatability of experiments carried out under what would appear to be near-identical operating conditions. By pre-conditioning under rich conditions highly repeatable experiments were achieved. The results were combined to give a detailed picture of catalyst dynamics at pre-, mid- and post-catalyst locations, and provide insight into catalyst and (non-ideal) exhaust gas oxygen sensor behavior.*

INTRODUCTION

The dynamic behaviour of the exhaust gas aftertreatment system is widely recognized as having a significant impact on tailpipe emissions. One avenue of research has therefore focused on modeling this behaviour, either in terms of the detailed chemical kinetics of the system, Oshawa *et al*. (1998), or in the form of much simpler control-oriented real-time models based on oxygen storage dynamics, Brandt *et al*. (1997), Peyton Jones *et al*. (2000), Balenovic *et al*. (2001). The former approach provides useful insight for catalyst design, while the latter provides a basis for the on-line optimization of catalyst operation, diagnostics, and control. An equally important area of research, however, concerns the experimental characterization of the catalyst. Indeed, such experiments are generally required in order to identify the parameters of a catalyst model or to validate the model predictions.

Previous experimental studies of 3-way catalyst behaviour have characterized the catalyst oxygen storage dynamics and the impact of these dynamics on conversion efficiency, Hepburn *et al*. (1992), Germann *et al*. (1996), Jackson *et al*. (1999). Similar work has also shown how the conversion efficiency can degrade either due to short term reversible catalyst deactivation, Campbell *et al*. (2000), Peyton Jones *et al*. (2002), or due to longer term / permanent deactivation caused by catalyst age or poisoning, Hepburn *et al*. (1992). Previous experimental work has also highlighted the effects of the dynamically changing exhaust gas composition seen downstream of the catalyst upon the Exhaust Gas Oxygen (EGO) sensors used for feedback control or for diagnostics purposes. If these effects are ignored, they can compromise the performance of the control and diagnostic system, Peyton Jones *et al*. (2003), but if the cross-sensitivity to gases other than oxygen are treated appropriately then they can be exploited in order to extract more information about the behaviour of the system, Aukenthaler *et al*. (2004), Peyton Jones *et al*. (2006).

The present study extends this work using a comprehensive set of fast-response instrumentation and production sensors, and by recording data from mid-brick, as well as pre- and post-catalyst locations. The issue of sensor location and sensor type is critical in real-time catalyst control and On Board Diagnostic (OBD) applications *(see Sect. 1)*. Both wide-ranging Universal Exhaust Gas Oxygen (UEGO) sensors and switching-type Heated Exhaust Gas Oxygen (HEGO) sensors were therefore installed at each sampling location and the dynamic gas composition at these points was measured using fast response gas analysers. Since production EGO sensors are known to have a strong cross-sensitivity to hydrogen, a hydrogen mass spectrometer was also used to measure the hydrogen concentration.

The hydrogen mass spectrometer is a single channel device and the fast response gas analyzers are two channel devices. To obtain measurements at the three desired locations therefore required the experiments to be repeated with different hydrogen and fast gas analyzer configurations in each case. Difficulties in obtaining repeatable results in an otherwise very tightly controlled experimental environment highlighted the existence of a new catalyst memory / dynamic effect which is reported in this paper. The overlay of experiments (once repeatable results had been achieved), also provides a very detailed picture of catalyst and sensor transient response as changes in feed-gas propagate through the catalyst.

The paper is organized as follows. The original motivation for the study, and the importance of production sensor location and type is discussed in Section 1. Experimental details are described in Section 2. Initial test results are presented in Section 3 and the results of nominally identical repeat experiments are discussed in Section 4. These experiments show significant differences from the results of Section 3, and the dependence of these differences on catalyst precondition is investigated in Section 5. The results, after repeatable conditions were obtained, are discussed in Section 6. Finally, brief conclusions are given.

1 FEEDBACK SENSORS: CONSIDERATIONS

The performance of catalyst control and diagnostic strategies depends critically on the type, location and accuracy of the sensor that is used for measurement and feedback. Advanced control schemes typically use wide-ranging UEGO sensors as the post-catalyst feedback sensor while production systems typically use narrow range HEGO sensors. Most UEGO-based strategies attempt to maintain the estimated catalyst oxygen level near the stoichiometric equilibrium state in order to maximize the time required to reach either rich or lean tailpipe emission breakthrough when subject to disturbances. Linear control strategies of this type have been proposed based on LQR by Ohata *et al*. (1995), H_∞ by Shafai *et al*. (1996), and IMC by Balenovic *et al*. (2001). Nonlinear model-based control formulations include those by Balenovic *et al*. (2002) and Fiengo *et al*. (2005). A multi-objective nonlinear model-based strategy that uses the oxygen storage capacity of the catalyst to optimize engine performance and fuel economy while preventing emission breakthrough is described in Muske and Peyton Jones (2006).

Although these strategies are able to optimize the response to large transients such as fuel cut-off during over-run or gear change flare, the system can become almost unobservable when the catalyst is at the desired stoichiometric equilibrium state. In this situation, pre-catalyst Air/Fuel Ratio (AFR) transients have very little impact on the post-catalyst response because they are attenuated by catalyst oxygen storage and release. The changes in post-catalyst AFR are therefore very small and difficult to detect with a UEGO sensor. By contrast, a HEGO sensor has a high gain in the stoichiometric region

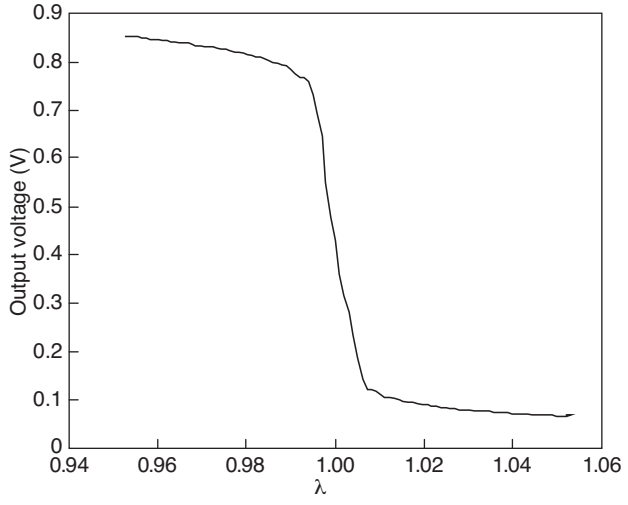

Figure 1

HEGO sensor response as a function of AFR, λ.

(as shown in *Fig. 1*) which provides more precise feedback at this specific operating point. It is also a lower cost sensor making its use attractive in production catalyst control systems. Its disadvantage, however, is rapid sensor signal saturation when subject to large AFR transients.

HEGO-based control strategies typically cycle the pre-catalyst Air Fuel Ratio across stoichiometry at a frequency determined during engine calibration or obtained through relay feedback from a post-catalyst HEGO sensor (Eastwood, 2000). The HEGO sensor relay feedback control scheme in Makki *et al*. (2005) is one example of a current production control system. Application of model-based control using a post-catalyst HEGO sensor is presented by Balenovic *et al*. (2006). A predictive functional control approach in which the HEGO relay control parameters are optimized online is described in Schallock *et al*. (2009). The use of relay control strategies is in some ways dictated by the switching nature of the HEGO sensor, but there is also evidence that cycling AFR may help reduce emissions (see Silveston, 1996 and the detailed experimental study documented in Cornelius, 2001).

One difficulty associated with relay-based control strategies, however, is the transport delay inherent in the exhaust system which can lead to larger perturbations of catalyst state than may be desirable, or even to emission breakthrough. Delay can be especially significant for multi-catalyst systems where the downstream catalyst is often far from the engine. For these reasons it is common to locate the feedback sensor either mid-brick (in single catalyst systems) or between bricks in multi-catalyst systems. These "mid-brick" locations are advantageous from a control perspective because they reduce the delay associated with the measurement. Any deficiencies in control performance at the mid-point can also be compensated for by the rear brick which is downstream of the sensor. However, mid-brick feedback is not desirable from an OBD perspective since the rear brick cannot be monitored with this configuration. In order to monitor the entire catalyst volume, either a third sensor must be installed or the feedback control sensor must be moved downstream of the entire catalyst. Cost considerations makes relocating the feedback sensor a more attractive option. Although this re-introduces the delay, the large perturbations in catalyst state associated with delay in relay based control can be mitigated to some extent using strategies such as the pulse-width modulated control described in Peyton Jones *et al*. (2010).

A further consideration when using HEGO or UEGO sensors for feedback control and diagnostics is the dynamically changing gas-composition-induced bias experienced by these sensors when used in mid- or post-catalyst applications. Despite their name, Exhaust Gas "Oxygen" sensors have cross-sensitivities to other gas components, Germann *et al*. (1998), Buglass *et al*. (1998). This cross-sensitivity results in part from imperfect equilibration at the platinum electrodes of the sensor, and partly from differences in diffusion rate of the different gas components as they diffuse into the detection cavity. Small molecules, such as hydrogen, diffuse more quickly and are therefore over-represented at the sensing electrode causing (in the case of hydrogen) the sensor to read richer than true. In engine-out applications, where gas composition is a fairly static function of AFR, these effects can be treated using a simple calibration curve such as that shown in Figure 2. In mid- or post-catalyst applications, however, the gas composition changes dynamically as a function of the reactions taking place on the catalyst brick, and it becomes much harder to separate true changes in AFR from changes due to gas composition effects.

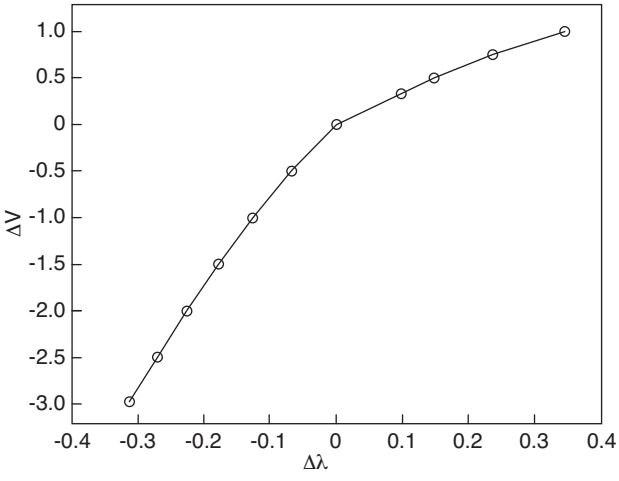

Figure 2

UEGO sensor calibration curve.

In order to address all these issues, it is helpful to have a detailed picture of how both the catalyst and the sensors respond to changes in AFR – both at the mid-brick location, and at the post-catalyst location. The present study was originally aimed at obtaining this data, but it also revealed previously unreported persistent catalyst memory effects.

2 EXPERIMENTAL DETAILS

The converter used in this experimental study was a two-brick Pd/Rh catalyst that had been dynamometer-aged to 50 000 miles. The catalyst was positioned to simulate an under-floor device in the exhaust system of a 2.0 litre Ford I4 gasoline engine. A photograph of the engine-catalyst system is shown in Figure 3. The catalyst was subjected to a defined sequence of AFR perturbations generated by the engine control system. In order to be able to command a highly repeatable profile for the AFR perturbations, the rapid prototyping capability of the Electronic Control Unit was used to embed a signal generator in the software of the control strategy. The user can adjust the parameters of the signal generator over a Controller Area Network (CAN), although for the data presented in this paper, only a square wave was used. The commanded signal is then fed to a recently-developed dead-time compensated AFR control strategy (Franceschi *et al*., 2008) whose task is to ensure the engine-out/catalyst-in AFR follows the desired target despite the large time-varying delay through the engine.

For the experiments presented in this study, the engine operating condition was set at 2 500 rpm and 52% load. Catalyst brick temperatures were approximately 475°C on average. Low sulfur, summer-blend, fuel was supplied by ExxonMobil Research and Engineering Company. This test fuel is 92 (R+M)/2 octane, contains no oxygenated compounds, and has a sulfur content less than 2 ppm (mg/kg).

Also seen in Figure 3, is the instrumentation used to monitor the catalyst response to the AFR perturbations. The instrumentation includes both fast response gas analysis equipment (for measuring the individual components CO, CO_2, NO, HC and H_2), as well as low-cost production EGO sensors whose behaviour is important because they provide the inputs to the control and diagnostic system. Pairs of HEGO and UEGO sensors are positioned upstream, downstream and mid-brick respectively so that the behaviour of these sensors and their interaction with the catalyst dynamics can be studied.

The use of fast response gas analyzers is necessary since the instruments must respond faster than the catalyst dynamics of interest. The rise times of this equipment are 7 ms or less, although the hydrogen analyzer rise time is slightly slower at 300 ms. The hydrogen analyzer is also a single channel instrument, but a solenoid control valve can be used to switch the gas sampling point to different locations. By repeating the same experiment with the sampling point switched to a different location, a good approximation to the gas concentrations at all three points of interest can be obtained.

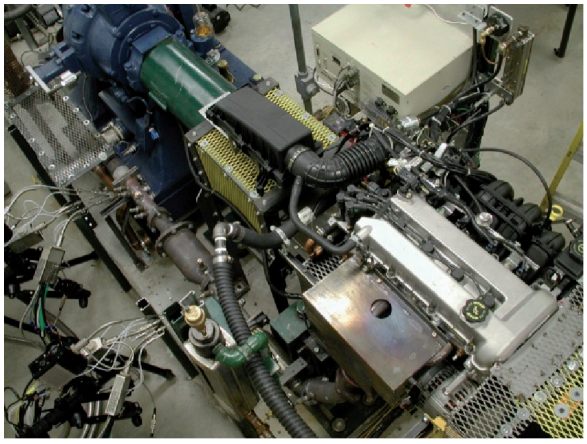

Figure 3

Photograph of the engine-catalyst system.

The other fast response analyzers are dual channel instruments so simultaneously recorded data can be gathered from pre- and post-catalyst locations. To obtain the mid-brick information, however, the downstream sampling point of each instrument is moved mid-brick and the experiment repeated. The different sampling configurations are summarized in Table 1 and denoted A, B, and C. It is important to note that many measurements are common across the different configurations. A comparison of the other signals, which are common to both configurations, can therefore be used to check the repeatability of the experiments.

TABLE 1

Configuration of gas sampling locations

Configuration →	A	B	C
Dual channel analyzer: Ch 1	Pre	Pre	Mid
Dual channel analyzer: Ch 2	Post	Post	Post
Single channel H_2 analyzer	Pre	Post	Mid

3 FIRST EXPERIMENT (A)

In this experiment, the catalyst is pre-conditioned lean and is then subjected to step transitions in feedgas AFR at 60 second intervals. The AFR step amplitude was +/– 5% relative to stoichiometry. The results, shown in Figure 4 are fairly typical for an initially oxygen-saturated catalyst. Immediately following the lean-rich transition (t = 10 s until t = 11.3 s), the oxygen stored on the catalyst is released and combines with the rich incoming mixture to give low levels of post-catalyst

CO and HC, and correspondingly high levels of CO_2. The post-catalyst AFR is at stoichiometry, suggesting that the reductants are fully oxidized and that the oxygen release rate is limited only by input feedgas demand.

As this process continues, however, the oxygen release rate becomes "supply", rather than "demand", limited (t = 11.3 s until t = 16 s). The catalyst is no longer able to satisfy the oxygen deficiency in the feedgas and emissions levels rise because the incoming mixture is only partially oxidized. These changes are also reflected in the post-catalyst AFR signal which falls towards the pre-catalyst AFR level.

As the catalyst reaches its "depleted" equilibrium state, the oxygen storage / release rate becomes zero (at around t = 16 s). Theoretically, pre- and post-catalyst AFR signals should then become identical to one another since the oxygen storage/ release rate $\dot{\theta}$ is given by:

$$\dot{\theta} = \dot{m}_f K_\lambda (\Delta\lambda_{pre} - \Delta\lambda_{post}) \quad (1)$$

where $\dot{m}_f$ denotes the fuel mass flow rate, K_λ is a constant and $\Delta\lambda$ is a measure of the oxygen excess or deficiency in the gas relative to stoichiometry:

$$\Delta\lambda = \lambda - 1; \qquad \lambda = \frac{actual\ AFR}{AFR_s} \quad (2)$$

The apparent difference between the pre- and post-catalyst AFR signal during the extended rich period in Figure 4a is due to the UEGO sensor's strong cross-sensitivity to changing concentrations of hydrogen (Germann *et al*., 1998; Buglass *et al*., 1998) rather than a real difference in the true AFR. Under oxygen depleted conditions, the catalyst promotes the water-gas shift reaction:

$$CO + H_2O \rightleftharpoons CO_2 + H_2 \quad (3)$$

which alters the balance between CO and H_2 without otherwise changing the AFR. Since hydrogen is a small molecule relative to oxygen it diffuses approximately four times faster through the diffusion barrier of the UEGO sensor causing the sensor to read richer than true and resulting in the apparent "overshoot" in the apparent AFR signal seen in Figure 4a at t = 16 s. This interpretation is strengthened by inspection of the hydrogen concentration signal seen in Figure 4g although the peak hydrogen level does not occur until t = 23 s. This temporal mismatch is attributed to the relatively slow (compared to the other instruments) response time of the hydrogen sensor, and transport delay and mixing associated with the sample line between the catalyst and the instrument. The true peak hydrogen level is expected to correspond with the maximum "overshoot" in the UEGO signal at t = 16 s.

The slow, dynamic change in H_2, CO, HC, and the apparent AFR signal seen in the extended period following t = 16 s is due to reversible deactivation effects (Peyton Jones *et al*., 2002) which cause the catalyst surface to become less active with time until the AFR transitions lean again and the surface is regenerated. During the deactivation period, less hydrogen is generated *(Fig. 4g)* which in turn causes the AFR signal to shift upward as observed in Figure 4a. Conversion efficiencies also fall and corresponding increases in emissions are observed, *(Fig. 4c-f)*.

The steady state levels achieved in the period $60 < t < 70$ s demonstrates that the catalyst is still effective in reducing emissions even when oxygen release rates and all other dynamic effects are zero. The catalyst continues to bring the feedgas closer to chemical equilibrium: Incoming free oxygen and NO_x combine with CO, HC and H_2, resulting in lower steady state levels of all these components, and higher levels of CO_2, relative to the pre-catalyst composition. The effective water-gas shift reaction equilibrium constant which depends both on temperature and on the degree of catalyst surface deactivation, also no longer favours hydrogen production as strongly as it did during the initial lean-rich transient.

Rates of oxygen storage (rather than release) dominate the response on the rich-to-lean transition at t = 70 s. In this case, excess oxygen in the lean incoming gas flow is adsorbed onto the catalyst surface and re-oxidizes the bulk ceria. The effective downstream AFR is therefore held near stoichiometry for a period, although the plateau effect is not so clearly defined. Downstream emissions levels are low during this period, but NO levels then rise as the adsorption rate slows, and the stored oxygen approaches the "saturated" equilibrium from which the experiment began.

4 SECOND EXPERIMENT (B)

As mentioned in Section 2, the hydrogen analyzer used in experiment A is a single channel instrument. The pre-catalyst hydrogen trace shown in Figure 4g was therefore actually obtained from a repeat experiment, B, that was conducted with no change from A other than the relocation of the hydrogen analyzer upstream of the catalyst. Care was taken to ensure that all the experimental test conditions were tightly controlled to match those in experiment A, and the repeatability of the experiment was also checked by comparing all the other signals which are clearly duplicated in both tests. Though not shown, all the pre-catalyst gas concentrations measured in experiment B were found to be within 2% of the values observed in experiment A. This suggests that a high level of repeatability had been achieved. It was therefore somewhat surprising to discover that the post-catalyst signals were significantly different from those measured previously. Figure 5 shows a comparison of the all the post-catalyst signals recorded in the two experiments. As indicated above, the pre-catalyst signals show excellent repeatability but they are not shown in Figure 5 for reasons of clarity.

Inspection of Figure 5 shows that the response of all the signals repeats fairly closely during the oxygen depletion

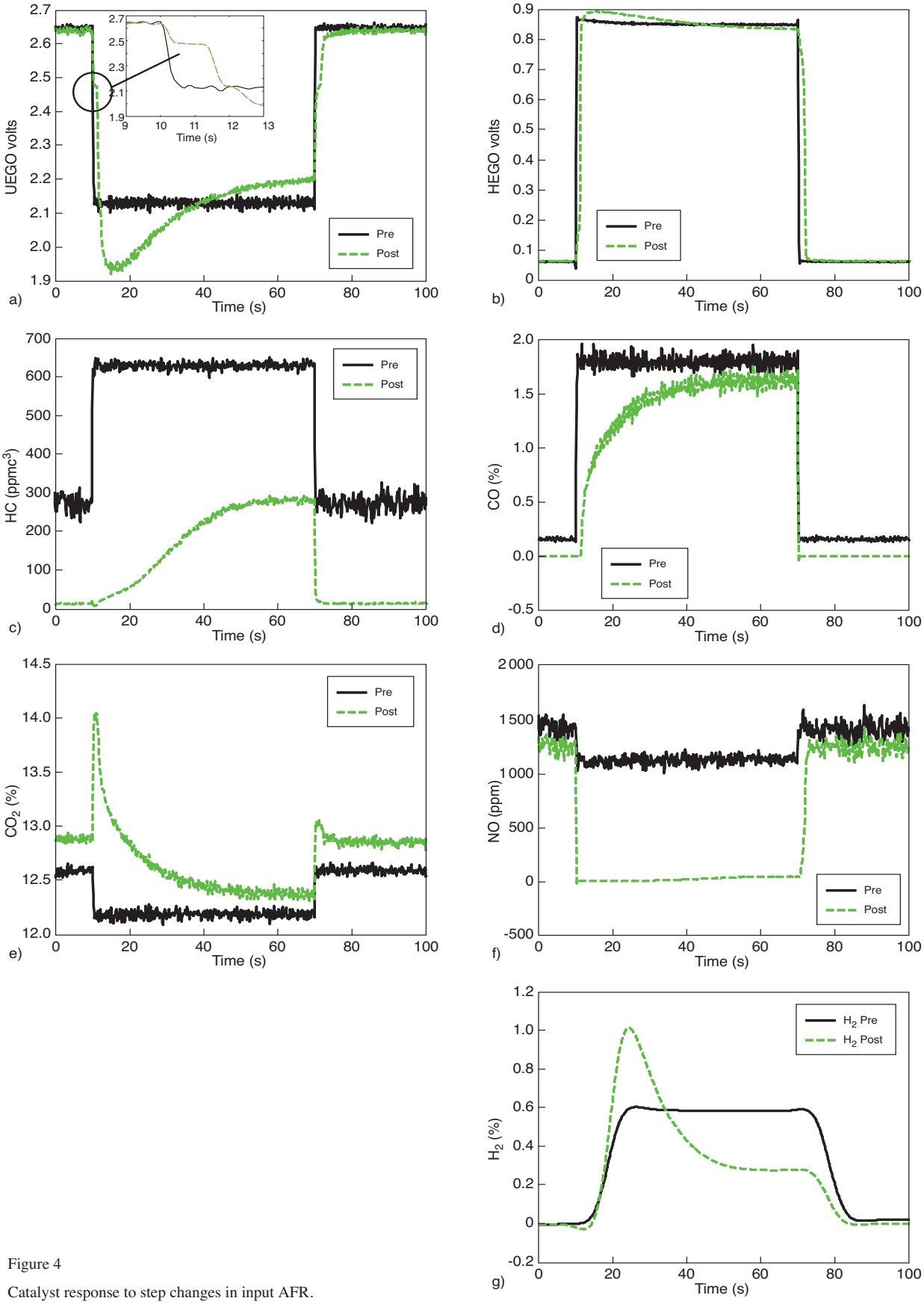

Figure 4

Catalyst response to step changes in input AFR.

phase. The significant difference in the response during the reversible deactivation period, however, suggests that the catalyst surface is more active in experiment A than it was in experiment B. Furthermore, the time constant of the deactivation process in B is significantly faster than in A.

At first it was suspected that some other experimental condition was responsible for these differences. The recorded engine operating conditions were checked and found to be highly repeatable. Catalyst brick temperatures were also compared and found to be within 0.6% of each other at the start of each experiment. However, other variables such as combustion air humidity were not recorded. To rule out the possibility that such variables could have affected the results, the two experiments were repeated again, one after the other, without stopping the engine or changing its operating point. This procedure did not change the previous observations. In fact, the data presented in Figure 5 is the result of one of these sequential tests, and it confirms the observations made earlier from data gathered on different days.

These results suggest that the differences between repeat experiments are due to the catalyst itself and that there is some previously unobserved catalyst memory effect which significantly affects conversion efficiency during the reversible deactivation dynamic portion of the response. Similar effects have been observed on longer timescales and attributed to sulfur in the fuel, but it should be noted that the fuel used in this study had very low sulfur content and the differences in response are observed on relatively short time scales. In the interests of brevity, only the repeatability of the measured AFR/UEGO sensor signal is discussed in the sequel, though this is strongly correlated to the other gas responses as seen Figures 4 and 5.

5 SEQUENTIAL EXPERIMENTS (A, B) AND THE EFFECT OF DIFFERENT PRECONDITIONS

In order to investigate the apparent memory effect, the pre-condition prior to the start of each experiment was closely examined. The original tests, performed on different days, were designed to have a 60 s lean pre-condition in order to fully saturate the catalyst with stored oxygen prior to the start of the tests. Because of the concern about possible slow memory / dynamic effects, this lean pre-condition period was extended first to 5 minutes, and later 9 minutes, prior to the start of each test. A diagrammatic representation of the applied AFR waveform for the two sequential experiments is shown in Figure 6. A period of near-stoichiometric operation preceded both tests during which time the gas analyzers were calibrated.

Extending the precondition period from 60 s to 5 minutes very slightly improved the repeatability of experiment B relative to experiment A, but thereafter further lean conditioning had no appreciable effect *(compare Fig. 7 and 5a)*. The most notable feature of these results is that even very extended periods of lean operation do not erase whatever catalyst memory effect causes the differences between the two experiments. This result is surprising because reversible catalyst deactivation dynamics generally build up under rich or rich-biased operation and are erased by a short period of regenerative lean operation (Campbell *et al*., 2000). Indeed, the lean pre-condition had been chosen precisely because it was believed to drive the catalyst to a better defined initial state.

Looking further back in the pre-condition history, the remaining difference in the prior condition of experiment A relative to B is the period of stoichiometric operation (prior to experiment A only) during which the gas analyzers were calibrated. During this period, zero and span calibration gases are injected into the exhaust to be re-sampled by the gas analyzer for calibration purposes. The calibration gases are also swept through the catalyst by the exhaust flow and it was thought that these gases could be the cause of the observed discrepancies between the two experiments.

The sequence of experiments A-B, together with the initial period of stoichiometric operation, were therefore repeated without calibrating the analyzers. The results were almost identical to those shown in Figures 5 and 7, suggesting that it is the period of stoichiometric operation itself, rather than the analyzer calibration process, that differentiates the two experiments.

To test this hypothesis, the sequence of experiments A, B were re-designed so that each had a period of stoichiometric operation prior to the nominal lean precondition. The AFR waveform for the sequence then has the form shown in Figure 8. As seen from the results *(Fig. 9)*, the two experiments now have very similar response time histories, confirming the importance of the period of stoichiometric operation for the repeatability of experiments. Although the test as a whole is now repeatable, it is interesting to note the differences between the first and second lean-rich step transitions within the test. On the first transition, which follows immediately after 5 minutes of lean operation, the UEGO sensor voltage falls to a lower value than it does on the second lean-rich transition. This behaviour suggests increased levels of hydrogen and catalyst activity for the first transition – an indication perhaps that complete catalyst regeneration from reversible deactivation effects requires longer periods (> 60 s) of lean operation than was previously assumed.

There was some concern that the need for a period of stoichiometric operation, though beneficial in some respects (as seen above), could also introduce some ambiguity in the initial catalyst state. If, for example, the AFR has a small lean offset from stoichiometry, then the catalyst will approach its oxygen saturated condition during the nominally "stoichiometric" period. Conversely, if a small rich offset or bias exists during this period, then the catalyst will tend towards its oxygen depleted condition. To remove this ambiguity, further experiments were performed using a rich biased

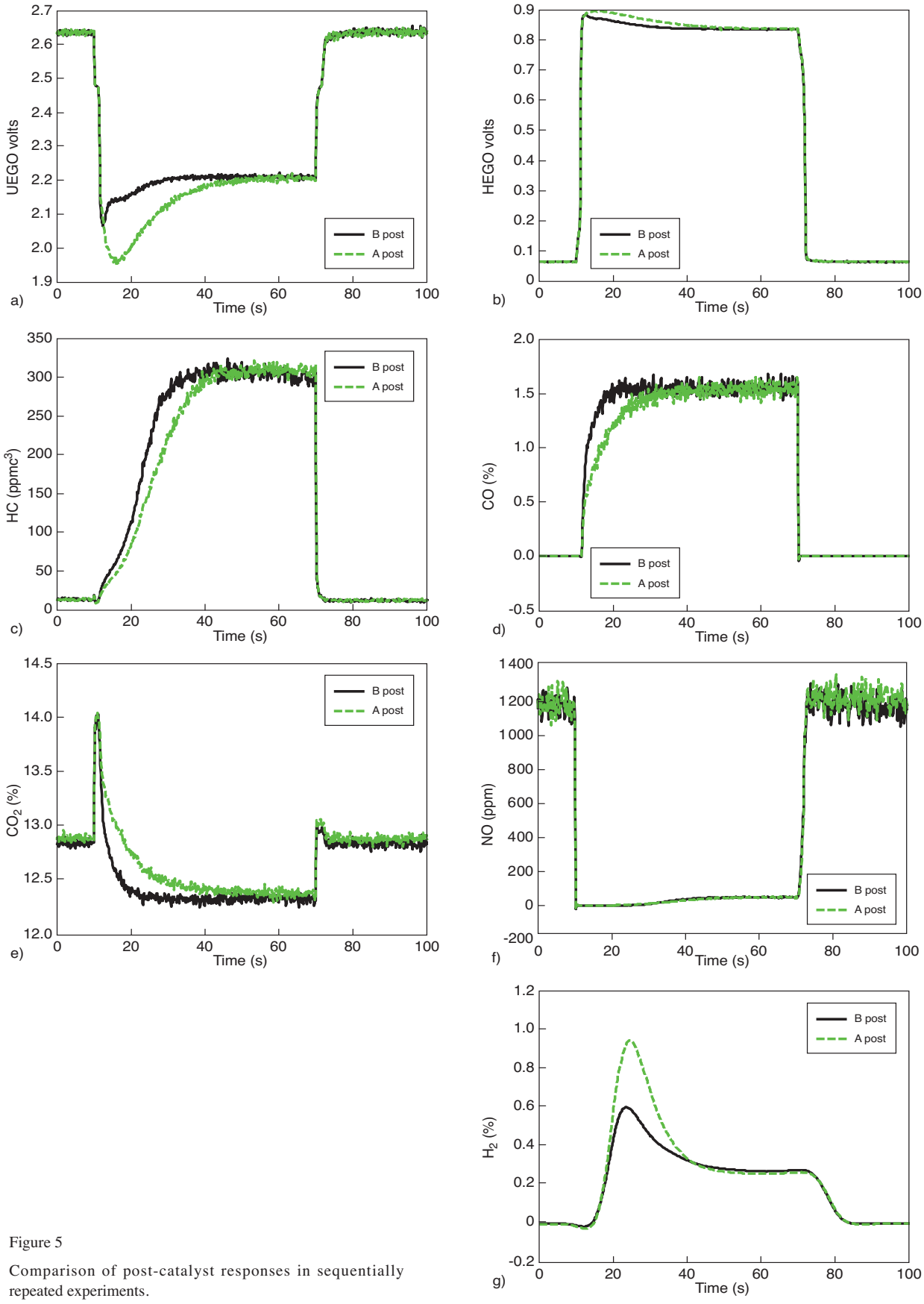

Figure 5

Comparison of post-catalyst responses in sequentially repeated experiments.

Figure 6

Test sequence with extended lean preconditions.

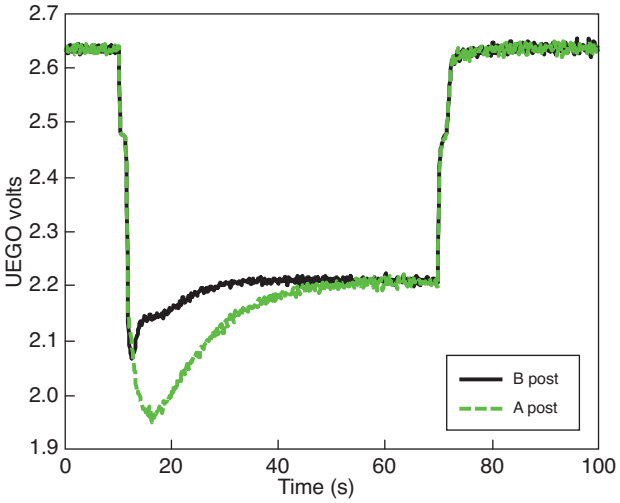

Figure 7

UEGO sensor response after extended lean precondition.

Figure 8

Test sequence with stoichiometric preconditions.

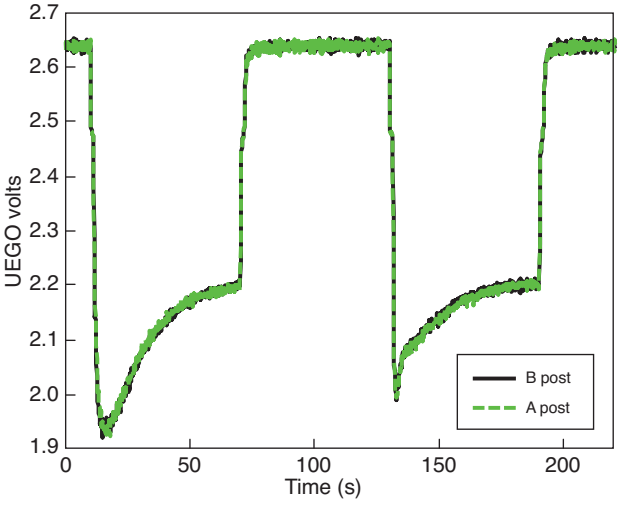

Figure 9

UEGO sensor response after stoichiometric precondition.

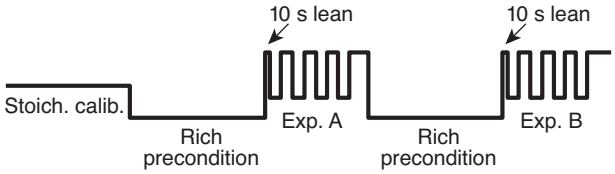

Figure 10

Test sequence with rich preconditions.

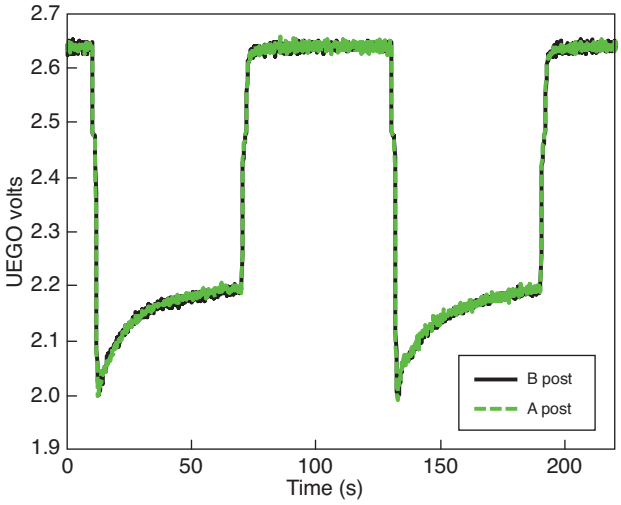

Figure 11

UEGO sensor response after rich precondition.

pre-condition to replace the period of stoichiometric operation and the "lean-precondition" periods of the earlier tests. The AFR waveform for the sequence of two tests then has the form shown in Figure 10, where the 10 s lean period at the start of the test relates to the details of triggering the data acquisition system(s) rather than any intentional conditioning of the catalyst. The results *(Fig. 11)* show that the experiments are again very repeatable, suggesting that rich operation (as well as operation at stoichiometry) also erases persistent catalyst memory effects. Inspection of Figure 11 also shows that the response to the first, second, and subsequent lean-rich transitions within any test are now more similar to each other. This suggests that the catalyst state, including the reversible deactivation dynamic state, is better defined under rich preconditions than under lean pre-conditions. All the results reported in the sequel have therefore used a rich precondition period as the default for giving reliable and repeatable results.

6 PRE-, MID- AND POST-CATALYST RESPONSE

Having developed a procedure to obtain repeatable results, it is then possible to overlay the data from different measurement

configurations (A, B, C in *Tab. 1*) in order to construct a complete picture of the catalyst response at pre-, mid- and post-catalyst locations. The results, shown in Figure 12, are similar to those of Figure 4 only now with the addition of the mid-brick signals.

Figure 12a for example shows (on the enlarged inset) the UEGO sensor response immediately following the lean-rich transition at t = 10 s. The "demand limited" stoichiometric plateau observed in the mid-brick signal is much shorter than in the post-catalyst signal because the first brick alone cannot release oxygen at a rate sufficient to bring the rich incoming feedgas to a stoichiometric equilibrium. The spike in mid-brick CO_2 generation *(Fig. 12e)* is therefore more short-lived, and the mid-brick CO and HC concentrations start rising earlier. The release of oxygen by the first brick, though rate limited, does however continue for some time (until t = 12.5 s) as witnessed by the relatively gradual decline of the mid-brick UEGO signal.

This reduces the demand for oxygen placed on the second brick which is able to maintain a stoichiometric output composition (*i.e.* very low levels of HC and CO) until about t = 11.25 s. After this time, however, the post-catalyst AFR falls quite sharply (more rapidly than observed in the mid-brick signal), suggesting that the second brick has a smaller oxygen storage capacity. This is quite possible since the two bricks do not have the same formulation. Oxygen release from both bricks appears to end at about the same time, (approximately t = 12.5 s).

The remaining section of the rich-region response is dominated by reversible catalyst deactivation effects. Figure 12g for example shows the hydrogen concentration resulting from the water-gas shift reaction equilibrium. As noted previously, there is some temporal mismatch between the hydrogen signal and the rest of the data set due to sample line delay, mixing, and the slower response time of the instrument. However, the effect of reversible deactivation is still clearly visible; hydrogen concentrations peak shortly after the lean-rich transition, but then decay as the catalyst surface becomes less active. The peak mid-brick hydrogen level is similar to the pre-catalyst level but still significantly overshoots the steady state mid-brick level. Post-catalyst hydrogen concentrations peak at levels that are higher than pre-catalyst, but also decay to similar levels as exist mid-brick. In general, post- and mid-brick levels tend to converge in steady state as both bricks help transform the feedgas towards its chemical equilibrium.

These observations are consistent with the rich-region UEGO and HEGO traces recorded in Figure 12a,b. In theory pre-, mid- and post-catalyst AFR should be identical once oxygen storage and release effects have reached steady state (*i.e.* after t = 12.5 s). The differences observed between the pre-, mid- and post-catalyst signals during the long time period $12.5 < t < 130$ s are therefore dominated by sensor cross-sensitivity to hydrogen. The UEGO voltage drops to its lowest point during peak hydrogen production, and rises as the hydrogen levels decay. The mid- and post-catalyst UEGO sensors then appear richer, or leaner, than the pre-catalyst UEGO according to whether there is more, or less, hydrogen relative to the pre-catalyst level – even though AFR's are identical at all these points once storage dynamics have reached steady state.

The same cross-sensitivity to hydrogen can be seen in the HEGO sensor signals, *(Fig. 12b)*. Although, under rich conditions, the sensor is essentially saturated at around 0.9 V, the saturation voltage is seen to increase slightly during periods of peak hydrogen emission and it falls slightly as the hydrogen levels decay. The hydrogen cross-sensitivity of both the HEGO and UEGO sensor is important because it is easily misinterpreted as oxygen storage or release by the catalyst. This can degrade the performance of catalyst control or diagnostic strategies unless explicitly treated, Peyton Jones (2003).

The dynamics of CO oxidation into CO_2 can be seen in Figure 12d, e. After the initial low CO and high CO_2 spike during the oxygen release period, the response appears strongly correlated with hydrogen generation *(Fig. 12g)*, or the hydrogen-induced bias in the EGO signals *(Fig. 12a, b)*. This suggests that CO is oxidized by means of the water gas shift reaction, and that reversible deactivation of the catalyst surface results in the dynamic degradation of CO conversion efficiency that is observed. As expected, the mid-brick CO levels are higher than post-catalyst, but it is notable that the bulk of the CO reduction takes place on the first brick.

One other feature of note in Figure 12e, is the small spike on CO_2 generation that is observed immediately after the rich-lean transition at t = 70 s. Since feedgas levels of CO and HC are very low at this point, it suggests that some form of carbonaceous material is stored on the catalyst under rich conditions, and that this is released and oxidized once the AFR switches back lean. This storage mechanism could also occupy surface sites and therefore contribute to the reversible catalyst deactivation effects previously observed.

The hydrocarbon response of Figure 12c is interesting because it does not reach a steady-state condition during the 60 seconds of rich operation, but instead appears to rise almost linearly with time. The dynamics governing HC conversion, (after oxygen release has been completed), are therefore very slow, and could be modelled as a limited integrator. Such behaviour might possibly be associated with the carbonaceous storage mechanism discussed above and/or the steam reforming reaction. Whatever the mechanism, it is striking that the catalyst is able to reduce HC levels significantly even under rich, oxygen-depleted conditions. It is also notable that the bulk of this reduction occurs on the first brick, with a much smaller reduction occurring on the second brick.

Figure 12f shows NO levels pre-, mid- and post catalyst. As expected NO levels are high when lean, and low when rich.

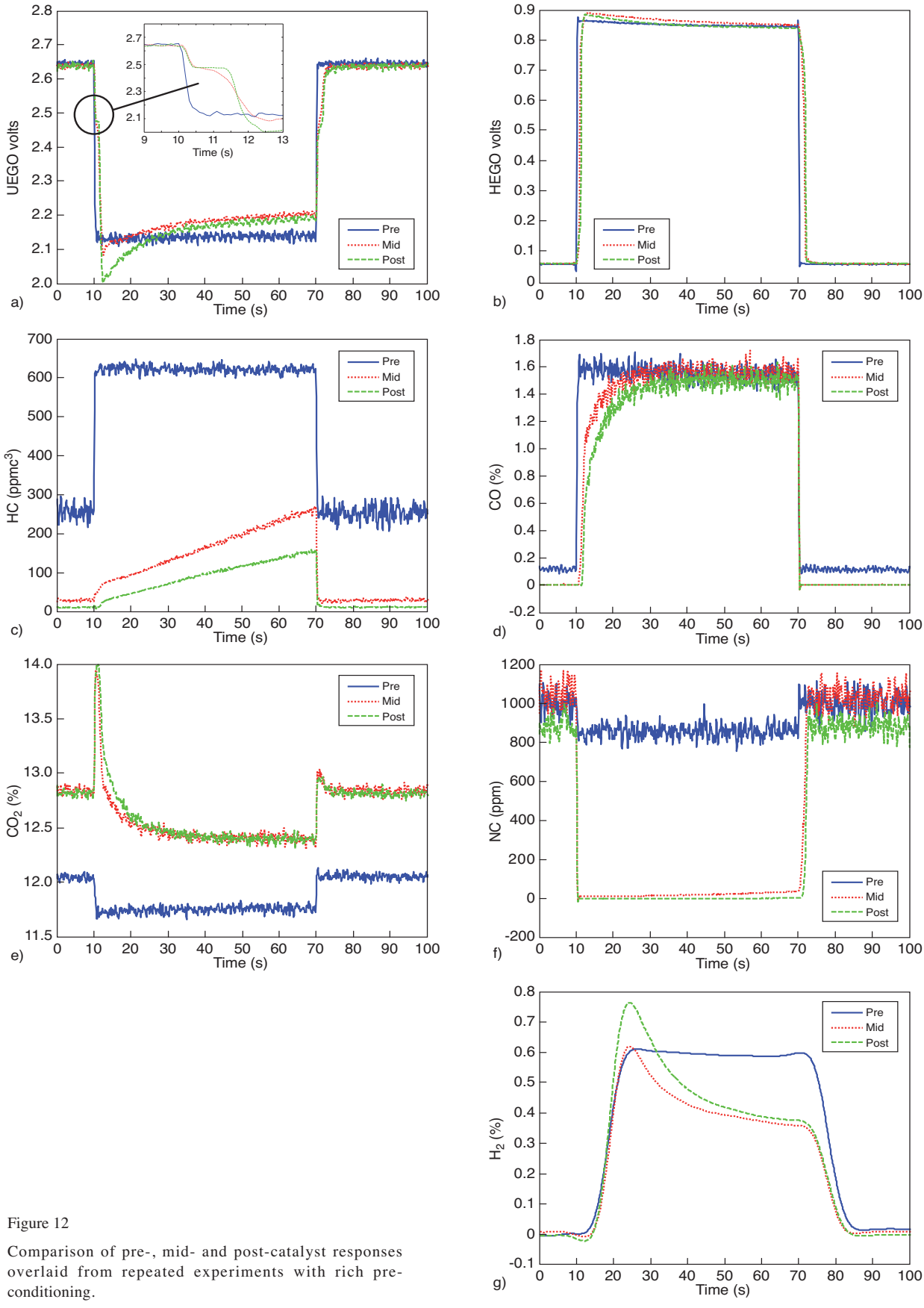

Figure 12

Comparison of pre-, mid- and post-catalyst responses overlaid from repeated experiments with rich pre-conditioning.

There are, however, some interesting differences between the mid-and post-catalyst signals. A small increase in mid-brick NO can be observed during the rich period of operation, and this may be attributable to reversible catalyst deactivation. However, a similar increase is not observed in the post-catalyst signal suggesting that the second brick is still able to reduce NO effectively. It is also noticeable that the post-catalyst sensor reads slightly lower than the mid-brick sensor under lean conditions. One reason for this might be a lack of repeatability in the calibration of the sensor (recall that the same sensor was used in different experiments, moving it from a post-catalyst to a mid-brick location). Another possibility, however, is that some oxidation of NO to NO_2 occurs on the second brick. Since the sensor measures NO rather than NO_x, this would slightly reduce the post-catalyst signal.

CONCLUSIONS

The dynamics of three-way catalytic converters have a profound impact on the conversion efficiency of a gasoline aftertreatment system. Although the effects of catalyst oxygen storage dynamics are widely recognized, other dynamics such those due to reversible catalyst deactivation can have a slower but nevertheless important effect on conversion efficiency. These effects should not be neglected since they build up over time, even under rich-biased "cycling" conditions as opposed to the unrealistically prolonged rich operation considered here.

The work described in this paper has also shown that slow dynamics/catalyst memory effects can persist even after extensive periods of lean operation. This is in contrast to prior expectations where extended lean conditions were thought to drive the catalyst to a well defined state – fully saturated with oxygen and fully regenerated after any rich-operation-induced reversible deactivation. In fact, the work presented here shows that the initial catalyst state is more repeatably defined after preconditioning with stoichiometric or rich operation.

The ability to conduct repeatable experiments is an essential pre-requisite for investigations into catalyst and sensor dynamics. In this work, data from repeatable experiments, with the sensors positioned at different locations, were overlaid in order to obtain a more complete picture of the gas composition pre-, mid- and post-catalyst. Some initial discussion of the results have been presented. However, further work is needed in order to model and analyze the chemical kinetic mechanisms underlying the observed system behaviour, including the mechanisms underlying the persistent catalyst memory effects and reversible catalyst deactivation dynamics that have been highlighted in this paper.

ACKNOWLEDGMENTS

The support of Ford Motor Company, Johnson Matthey, ExxonMobil, and the Briar Hill Foundation is gratefully acknowledged. Villanova professor, Kenneth Muske, died in April 2010, but he made a significant contribution to an earlier version of this paper. His inspiration and encouragement are gratefully acknowledged and deeply missed.

REFERENCES

1 Aukenthaler T.S., Onder C.H., Geering H.P. (2004) Aspects of Dynamic Three-Way-Catalytic Converter Behaviour Including Oxygen Storage, *IFAC International Symposium on Advances in Automotive Control*, Salerno, Italy, pp. 345-350.

2 Balenovic M., Backx A.C.P.M., Hoebink J.H.B.J. (2001) On a model-based control of a three-way catalytic converter, *2001 SAE World Congress*, *SAE paper* 2001-01-0937.

3 Balenovic M., Backx T., de Bie T. (2002) Development of a model-based controller for a three-way catalytic converter, *2002 SAE World Congress*, *SAE paper* 2002-01-0475.

4 Balenovic M., Edwards J., Backx T. (2006) Vehicle application of model-based catalyst control, *Control Eng. Pract.* **14**, 3, 223-233.

5 Brandt E.P., Wang Y., Grizzle J.W. (1997) A simplified 3-way catalyst model for use in on-board SI engine control and diagnostics, *ASME International Congress and Exposition*, Sixth ASME Symposium on Advanced Automotive Technologies.

6 Buglass J.G., Morgan T.D.B., Graupner J.O. (1998) Interactions Between Exhaust Gas Compositions and Oxygen Sensor Performance, *1998 SAE World Congress*, *SAE paper* 982646.

7 Campbell B., Farrington R., Inman G., Dinsdale S., Gregory D., Eade D., Kisenyi J. (2000) Improved Three-way Catalyst Performance Using an Active Bias Control Regeneration System, *2000 SAE World Congress*, *SAE paper* 2000-01-0499.

8 Cornelius S. (2001) Modeling and control of automotive catalysts, *PhD Thesis*, University of Cambridge.

9 Eastwood P. (2000) Exhaust Gas Aftertreatment, *Research Studies Press*, Baldock, England.

10 Fiengo G., Grizzle J., Cook J., Karnik A. (2005) Dual-UEGO active catalyst control for emissions reduction: design and experimental validation, *IEEE Trans. Control Syst. Technol.* **13**, 5, 722-736.

11 Franceschi E.M., Muske K.R., Peyton Jones J.C., (2007) An adaptive delay-compensated PID air fuel ratio controller, *SAE 2007 Transactions, Section 3: Journal of Engines*, **V116-3**, pp. 888-894, and also *SAE paper* 2007-01-1342.

12 Germann H.J., Taglaiferri S., Geering H.P. (1996) Differences in Pre- and Post Converter Lambda Sensor Characteristics, *1996 SAE International Congress and Exposition*, *SAE paper* 960335.

13 Hepburn J.S., Gandhi H.S. (1992) The relationship between catalyst hydrocarbon conversion efficiency and oxygen storage capacity, *1992 SAE International Congress and Exposition*, *SAE paper* 920831.

14 Jackson R.A., Peyton Jones J.C., Pan J., Roberts J.B. (1999) Chemical aspects of the dynamic performance of a three-way catalyst, *1999 SAE International Congress and Exposition*, *SAE paper* 1999-01-0312.

15 Makki I., Surnilla G., Kerns J., Smith S. (2005) Engine control and catalyst monitoring with downstream exhaust gas sensors, *United States Patent* 6904751.

16 Muske K., Peyton Jones J. (2006). Multi-objective model-based control for an automotive catalyst, *J. Process Control* **16**, 1, 27-35.

17 Ohata A., Ohasi M., Nasu M., Inoue T. (1995) Model based air fuel ratio control for reducing exhaust gas emissions, *1995 SAE International Congress and Exposition*, *SAE paper* 950075.

18 Oshawa K., Baba N., Kojima S. (1998) Numerical prediction of transient conversion characteristics in a three-way catalytic converter, *1998 SAE International Congress and Exposition*, *SAE paper* 982556.

19 Peyton Jones J.C., Jackson R.A., Roberts J.B., Bernard P. (2000) A simplified model for the dynamics of a three-way catalytic converter, *2000 SAE International Congress and Exposition*, *SAE paper* 2000-01-0652.

20 Peyton Jones J.C., Jackson R.A., Roberts J.B. (2002) The importance of reversible deactivation dynamics for on-board catalyst control and OBD systems, *SAE 2002 Transactions, Section 4: Journal of Fuels & Lubricants*, pp. 76-84, and also *SAE paper* 2002-01-0067.

21 Peyton Jones J.C., Jackson R.A. (2003) Potential & pitfalls in the use of dual EGO sensors for 3-way catalyst monitoring & control, *Proc. Inst. Mech. Engs Part D* **217**, 475-488.

22 Peyton Jones J.C., Muske K.R. (2005) A novel approach to catalyst OBD, *SAE 2005 Transactions, Section 4: Journal of Fuels and Lubricants*, **V114-4**, pp. 44-45, and also *SAE paper* 2005-01-0024.

23 Peyton Jones J.C., Muske K.R., Schallock R.W., Avis J.M. (2010) A pulse width modulation control scheme for three-way catalyst systems, *Proceedings of the 6th IFAC Symposium Advances in Automotive Control*, July 12-14, Munich, Germany.

24 Schallock R., Muske K., Peyton Jones J. (2009) Model predictive functional control for an automotive three-way catalyst, *SAE Int. J. Fuels Lubr.* **2**, 1, 242-249.

25 Shafai E., Roduner C., Geering H. (1996). Indirect adaptive control of a three-way catalyst, *1996 SAE International Congress and Exposition*, *SAE paper* 961038.

26 Silveston P. (1996) Automotive exhaust catalyst: is periodic operation beneficial? *Chem. Eng. Sci.* **51**, 10, 2419-2426.

Final manuscript received in February 2011
Published online in September 2011